ELSEVIER

Sensors and Actuators 80 (2000) 155–162

SENSORS AND ACTUATORS A PHYSICAL

www.elsevier.nl/locate/sna

An integrated MEMS three-dimensional tactile sensor with large force range

Tao Mei [a], Wen J. Li [b,*], Yu Ge [a], Yong Chen [a], Lin Ni [a], Ming Ho Chan [b]

[a] *State Key Laboratories of Transducer Technology, Institute of Intelligent Machines, Chinese Academy of Sciences, Hefei, Anhui 230031, China*
[b] *Advanced Microsystems Laboratory, Department of Mechanical and Automation Engineering, The Chinese University of Hong Kong, Shatin, New Territories, Hong Kong, China*

Received 30 March 1999; accepted 19 July 1999

Abstract

An integrated three-dimensional tactile sensor with robust MEMS structure and soft contact surface suitable for robotic applications was developed. The sensor has a maximum force range of 50 N in the vertical direction and ± 10 N in the x and y horizontal directions. The tactile sensor includes 4×8 sensing cells each exhibiting an independent, linear response to the three components of forces applied on the cells. By finite element analysis, optimal cell structures and piezoresistor positions were determined. Post bulk-micromachining was performed on foundry-fabricated CMOS chips to produce the sensor cells. With neural network training, the tactile sensor produced reliable three-dimensional force measurements and repeatable response on tactile images. Design analysis, fabrication procedures, and experimental results are presented in this paper.

Keywords: Tactile sensing; Tactile imaging; MEMS sensors; Robotic sensing; MEMS and CMOS integration

1. Introduction

Many tactile sensors have been developed to provide tactile sensing abilities for tele-operational manipulators, intelligent robots, and haptic interfaces [1,2]. These tactile sensors can detect normal forces applied on the tactile pixels for gripping force control and generate tactile images for gripping positioning and object recognition. However, besides acquiring tactile images and normal forces, knowledge of tangential forces is also critical for force control and slide-prevention during gripping to task success, and therefore, three-dimensional tactile sensors are needed.

Several three-dimensional tactile sensors have been developed using piezoresistive [3], capacitive [4], and optical [5] sensing elements. Some of these tactile sensors were fabricated by MEMS technology that integrated sensing elements and pre-processing circuits for compactness, but were too weak and fragile for most applications. For example, the force range of a capacitive tactile pixel is only 0.01 N [4]. Other tactile sensors that were not produced by MEMS technology are typically bulky (for example, a CCD camera is needed in an optical tactile sensor [5]) or have limited spatial sensing resolution.

Nonrobustness to the applied forces or bulkiness of size prevents these three-dimensional tactile sensors to become potentially useful in robotic applications, especially for space robots. The reliability of space systems is a very important issue due to the high costs of space missions. Therefore, the robustness of tactile sensors must be improved to gain high component reliability. Furthermore, the costs of space missions are highly dependent on the payload weight (about US$260/g [6]), thus the tactile sensors must be compact or integrated to minimise the payload mass and match the size of compact space robots. Recent proposals for small/micro/nano satellites and micro rovers have raised the needs for space microrobots [7]. Although these microrobots truly require micron-scale sensors, millimeter-scale three-dimensional tactile sensors are urgently required by present space robotic systems.

We have developed a robust MEMS integrated three-dimensional tactile sensor with soft contact surface and large force range. The sensor uses an over-stop design to increase the robustness for overloading and has CMOS

* Corresponding author. Tel.: +852-2609-8475; fax: +852-2603-6002; e-mail: wen@mae.cuhk.edu.hk

0924-4247/00/$ - see front matter
PII: S0924-4247(99)00261-7

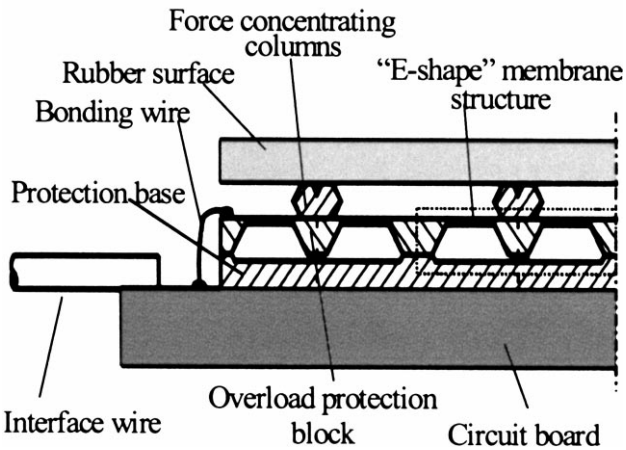

Fig. 1. Illustration of the cross-sectional view for the individual cells of the tactile sensor.

integrated piezoresistive sensing elements and on-chip data-reading circuitry to reduce total sensor volume.

2. Structural design

The integrated tactile sensor was constructed with five structural layers: rubber surface, force concentrating columns, sensing array, protection base, and circuit base as illustrated in Fig. 1. A 2-mm-thick rubber surface was used for absorbing shock and protecting the inner devices. It was made of highly elastic rubber used in fast-attacking type table tennis paddles. The rubber layer was glued on the top of the force concentrating columns by filling silicone rubber glue on the surfaces of the columns and the sensing array. The 703-type silicone rubber was used as the glue. It is a gel at room temperature, and by heating it to 50°C for 4 h, it becomes a soft rubber. This rubber glue has good electrical insulation property. The force concentrating columns were made by bulk silicon and positioned in the centre of the tactile sensing cells. Since the columns are surrounded by silicone rubber, a soft silicone rubber layer is formed around the columns. This silicone rubber glue layer provides large glue surface for the rubber surface and prevents moving friction on the sensing array surface. Therefore, the sensor may achieve more robustness while concentrating most of the distributed tactile forces onto the centre of the sensing cells in the tactile sensing array.

In the sensing array, there are 4×8 sensing cells that can detect three-dimensional forces. The sensing cell has an E-shaped square membrane structure (Fig. 1) fabricated by silicon bulk-micromachining. Strain induced by the applied forces on the membrane is sensed by three groups of integrated piezoresistors in the silicon membrane. By strain and stress finite-element analysis (FEA) of the E-shaped membrane, suitable positions for the piezoresistors were determined to obtain optimal circuit output for F_x, F_y and F_z. The FEA model for a single cell and its displacement contour due to 10 N F_z is shown in Fig. 2. The displacement at the centre of a 70-μm-thick membrane is ~ 20 μm due to 10 N force and hence the overload protection block (Fig. 1) was designed to be 20 μm above the protections base. The strain contour which indicates an asymmetric strain distribution on the membrane due to F_z is shown in Fig. 3. This asymmetric distribution is the key to using the membrane as the three-dimensional force sensor.

Locations of the piezoresistors on the membrane are shown in Fig. 4. When F_z is applied to the sensing cell, the stress and strain on the membrane where R_{x1}, R_{x2}, R_{y1}, and R_{y2} are located are theoretically equal, thus these piezoresistors have equal resistance change. Consequently, the output V_x and V_y of circuit C_x and circuit C_y have no

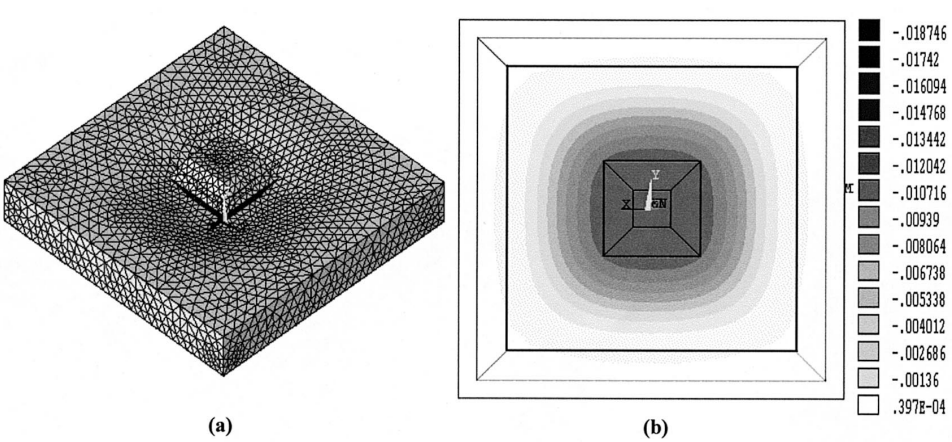

Fig. 2. (a) Mesh of the sensor cell for finite-element analysis. (b) Displacement contour of the sensor cell with 10 N force applied in the Z direction on the force concentrating column (see Fig. 1). The diaphragm thickness is 70 μm, the widest cross-section of the overload protection base and the force concentrating column is 1 mm × 1 mm. The sensing cell is 4 mm × 4 mm. As shown, the maximum deflection is ~ 0.0187 mm (18.7 μm) at the center of the diaphragm.

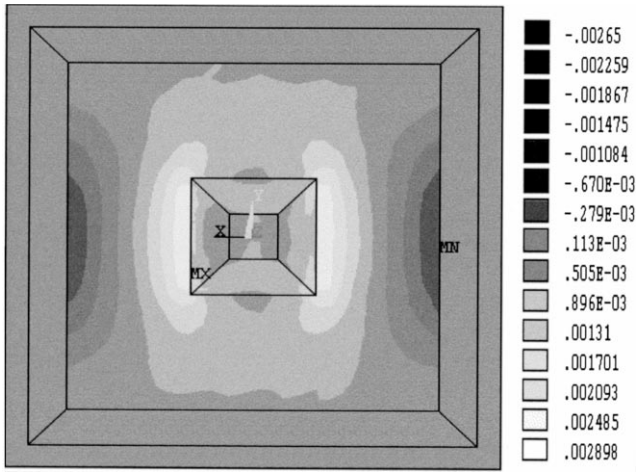

Fig. 3. Strain contour of the sensor cell diaphragm under 10 N force in the Z direction.

response to F_z. However, under the load of F_z, R_{z1} and R_{z2} are under compressive stress while R_{z3} and R_{z4} are under tensile stress. Thus, R_{z1} and R_{z2} decrease while R_{z3} and R_{z4} increase under F_z, and the output V_z varies accordingly. When F_x is applied on the sensing cells, R_{x1} is compressed while R_{x2} is elongated, and the output V_x varies correspondingly. In addition, R_{y1} and R_{y2} have the same resistance change in this case, therefore, C_y has no response to F_x. Also, the contributions from R_{z1} and R_{z2} are balanced in this case, since R_{z1} and R_{z2} are located on opposite but equal absolute value stress zones. For the same reason, the resistance change of R_{z3} and R_{z4} are balanced also. Therefore, V_z has no response to F_x. Similarly, when F_y is applied, V_y varies, but V_x and V_z have no response.

The protection base is a bulk-etched silicon substrate with predefined gaps to allow for the membrane deformation of the sensing cells, and is also designed to protect the membranes from excessive deformation. The maximum forces applied on the tactile sensor are 50 N in the Z direction and 10 N in the X and Y directions. These forces are distributed on all or some of the sensing cells.

Theoretically, every sensing cell in the tactile sensor must be designed to have the same force range as the tactile sensor, since the total tactile force may be concentrated on a single sensing cell in the worst case. However, if the worst-case scenario is taken into account, the sensitivity of sensing cells cannot be maximised. A trade-off was made in designing the force range for the sensing cells. Usually, as observed from human behaviour, larger contact area is needed to apply large forces to get a firm grip on an object. We have assumed that robots can work in the same manner, i.e., if the force on a single cell exceeds the force range of that cell, the excess force is

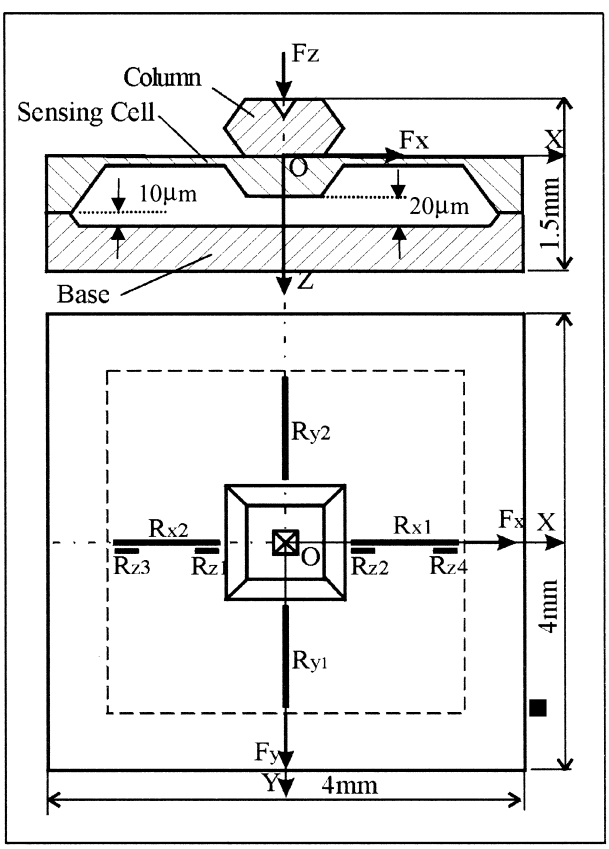

Fig. 4. Mechanical structure and piezoresistor locations of a three-dimensional force sensing cell.

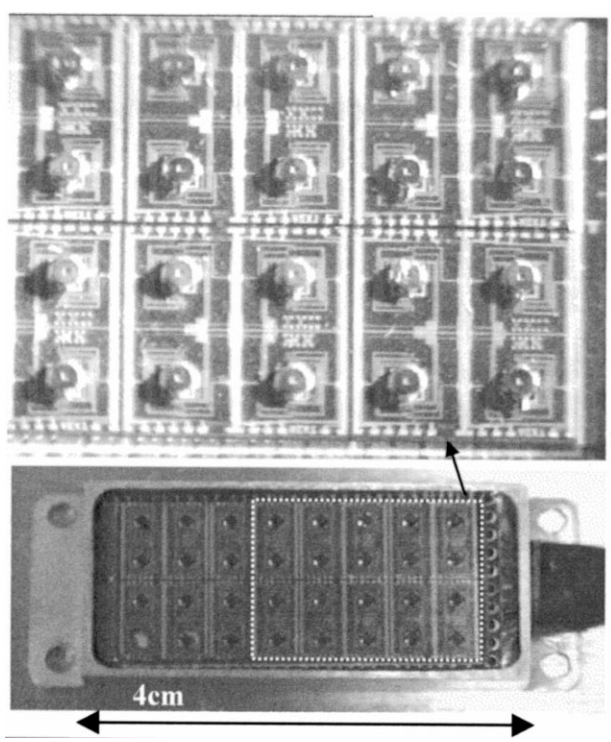

Fig. 5. Photograph of the tactile sensor without the rubber surface.

distributed to other cells on the tactile sensor. Therefore, we have designed the force range of the sensing cells to be 5 N in the Z direction and 1 N in other directions. Since the stress and deformation under F_z are much bigger than F_x and F_y, the predefined gaps on the protection base can prevent overloading on the membranes.

Finally, the above four layers and the circuit base are assembled into a metal case to form a complete tactile sensor with $20 \times 50 \times 7$ mm^3 total volume (Fig. 5). The circuit base is made of a PCB circuit board for off-chip wiring. There are four holes on this metal case for attaching the tactile sensor to robot gripper surface by screws. The sensing area of the tactile sensor is 16×32 mm^2 since each sensing cell is 4×4 mm^2.

3. Fabrication procedures

The tactile sensor was produced by four main processes: fabrication of small sensing cell array and the force overload-protection columns, micromachining of force concentrating column array, micromachining of protection base, and final assembling.

The fabrication of the small sensing cell array is the most important and difficult procedure since the array consists of integrated circuit and microstructures. If the total area of the sensing array is as large as 16×32 mm^2, the yield rate for a single chip containing all 32 fully functional sensing cells will be relatively low after many complex processing steps. Smaller sensing chips with 2×2 cells in an 8×8 mm^2 area were fabricated, and the total tactile sensing array was composed of eight small chips. Every small chip (Fig. 6) has independent integrated circuit elements including piezoresistors, sensing circuits (detect change of resistance), and analogue switches for data readout. The circuits for sensing, analogue switches, and data readout are shown in Figs. 7–9, respectively. The inter-chip and off-chip wire bonding contacts were patterned on every small chip, so any small chip could be placed in any position in the tactile sensing array.

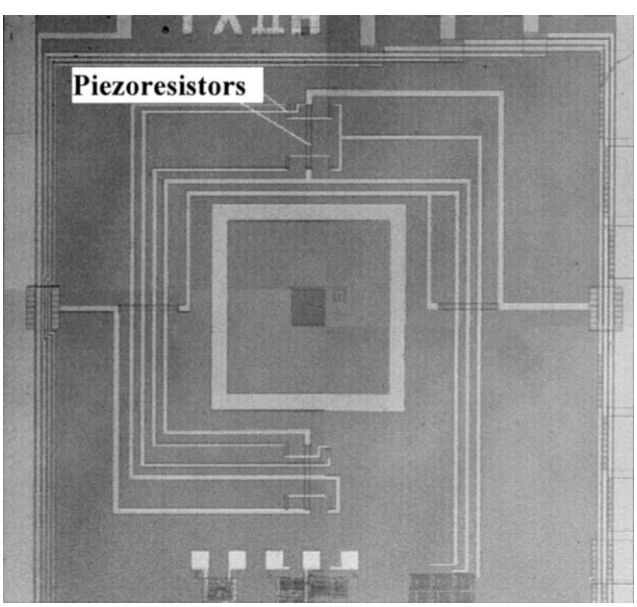

Fig. 6. Microphotograph of the piezoresistors and sensing circuits of a sensing cell.

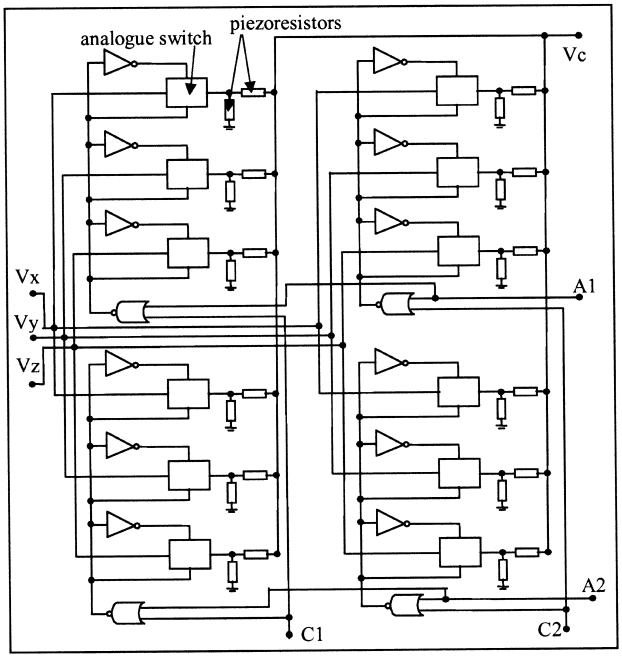

Fig. 7. Circuit diagram of the force-sensing circuit.

The CMOS integrated sensor-circuit chips of the sensing array were fabricated at the East China Research Institute of Optical Electronics using double-side polished 3-in. ⟨100⟩ silicon wafers. The doping concentration of the n-type silicon wafers is about 10^{15}/cm^3. The piezoresistors were formed by injecting B^+ with 5.5×10^{14}/cm^2

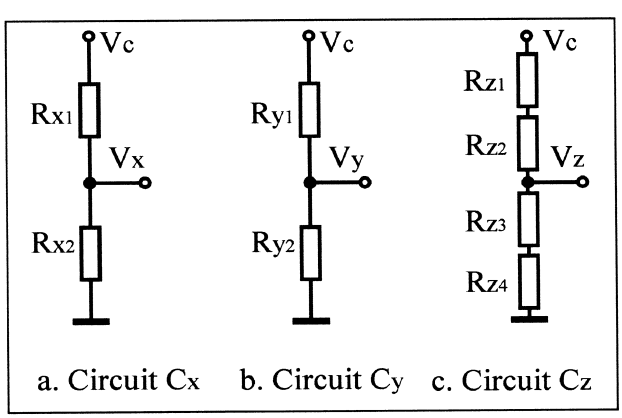

Fig. 8. Circuit diagram for the analogue switches (Vc is the excitation voltage for the sensor, io1 and io2 are the input and output of the switch, crla and crlb are the control signal. When both crla and crlb are low, io1 and io2 are connected, hence, allowing signals to pass through the switch).

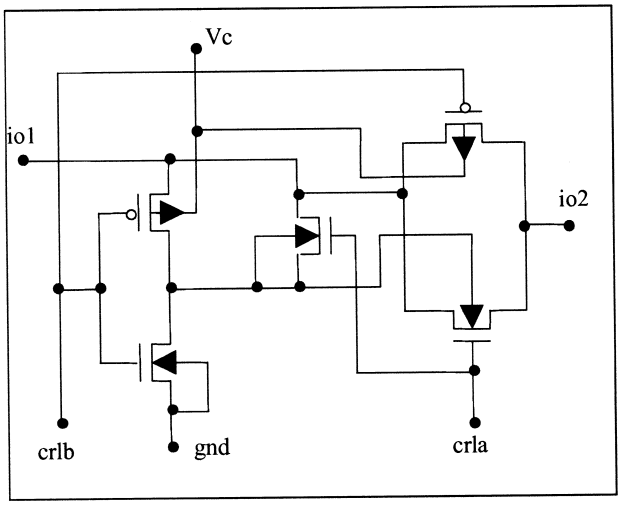

Fig. 9. Readout circuit for a 2×2 cell array (Fig. 10). The entire tactile sensor has eight of these 2×2 arrays. A1, A2, C1 and C2 are address lines that allows selection of signal from a cell in the 2×2 array by setting the address signals high or low. The entire sensor has 12 address lines: one for each of the eight 2×2 cell arrays and four (A1, A2, C1 and C2) that are commonly used by the eight arrays.

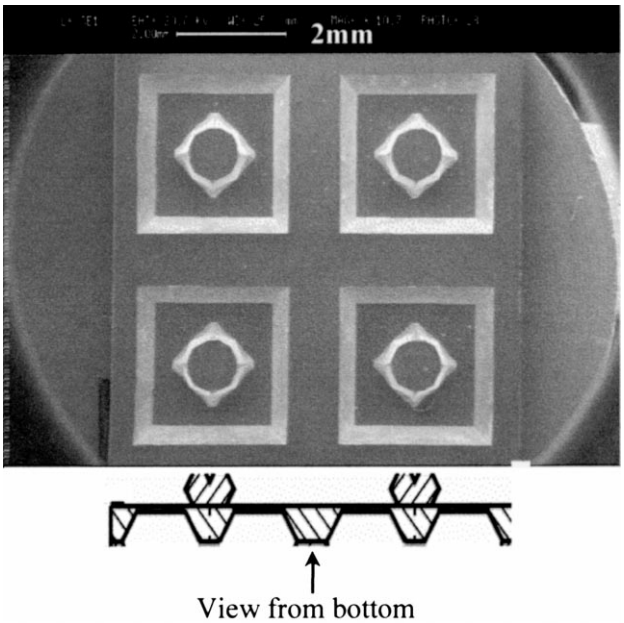

Fig. 10. SEM picture of the E-shaped membranes of four sensing cells.

dose, 100 μA beam-current, 40 keV for 35 s. The junction depths of the piezoresistors were diffused to about 1 μm by heating the wafers for 150 min under N_2 and 20 min under O_2 at 920°C. Standard CMOS process was used to make the detection circuits and the analogue switches.

A backside photolithographic procedure was followed to open etching windows for the E-shaped membranes. The CMOS circuits were protected and the chips were immersed in a 33% KOH solution at 76°C and time-etched to obtain 70-μm-thick membranes (Fig. 10). Finally, the silicon chips were cut to 8×8 mm^2 dice.

The force concentrating column array is initially composed of a frame with 4×8 columns connected by cantilevers. There are V-shape grooves at both ends of the cantilevers, so the cantilevers could be removed by applying a small force when the columns were glued to the center of the sensing cells. This way, the force concentrating columns could be easily handled, positioned and separated. The silicon column array was fabricated by the same bulk-micromachining process as the sensing cell array. The protection base was also made with silicon using the same technique.

The assembling process of the tactile sensor is described below. The procedure is illustrated in Fig. 11.

(a) Epoxy glue was coated on the protection base by thick-film printing technique, and eight selected small sensing arrays were placed on the protection base. A 50-g weight was applied on the top of the sensing array under 60°C for 4 h to get firm connection.

(b) Epoxy glue was printed on the center of the sensing array, and the force concentrating column array was aligned and pressed to the sensing array. Then, a 50-g weight was applied on the top of the column array under 60°C for 4 h to get firm connection.

(c) Small forces were applied to break the cantilevers, then 32 columns separately stood on the center of the sensing cells after the cantilever frame was removed.

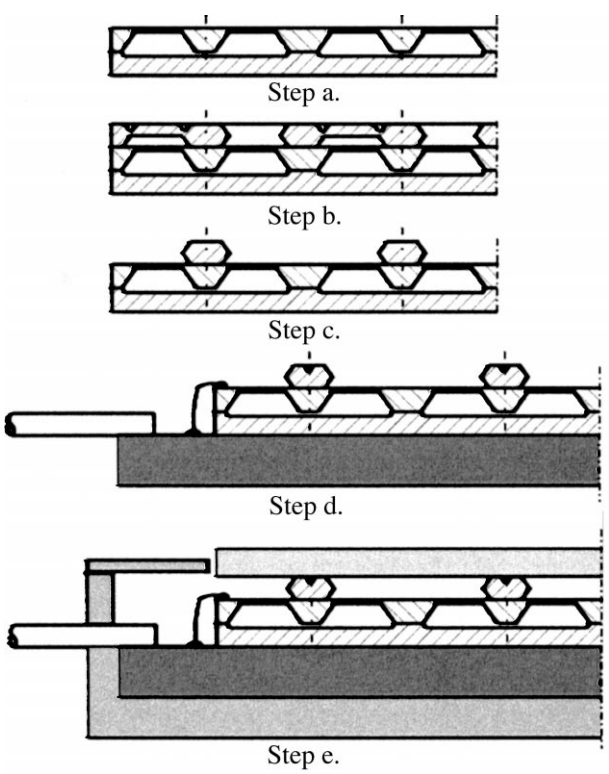

Fig. 11. The tactile sensor assembling process.

(d) The assembly was aligned, pressed and glued to the circuit base by the same method as in steps (a) and (b). Then, the inter-chip and off-chip wire bonding were performed.

(e) Finally, the assembly was fixed in the metal case by epoxy glue, and the rubber layer was adhered to the top surface by silicone glue. After 24 h of room-temperature glue drying, the fabrication process is complete.

As a note, the tactile sensing array has 19 off-chip lead wires: 12 address wires for cell selection, three output wires for cell force output, three power wires (+5 V, −5 V and ground wires) and a wire for reading temperature. If analogue switches were not integrated in the sensor chips, a total of 103 off-chip wires would be required for the tactile sensor, which would be a daunting task to implement.

4. Experimental results

The sensing cells were calibrated to determine their sensitivity before silicone rubber was used to cover them. The test set-up is shown in Fig. 12. A standard three-dimensional force sensor was used as the force reference, and was calibrated to 0.5% error by loading weights. The standard force sensor was fixed on a movable carriage in the *Z*-direction and could be moved down to apply a *Z*-direction force to the cells. The tactile sensor was fixed on an *X*–*Y* table. The forces on the *X* and *Y* directions could be applied by moving the tactile sensor in the *X* and *Y* direction when the head of the standard force sensor was pressed on the surface. A small hole was fabricated on the

Fig. 12. The sensor cell calibration set-up.

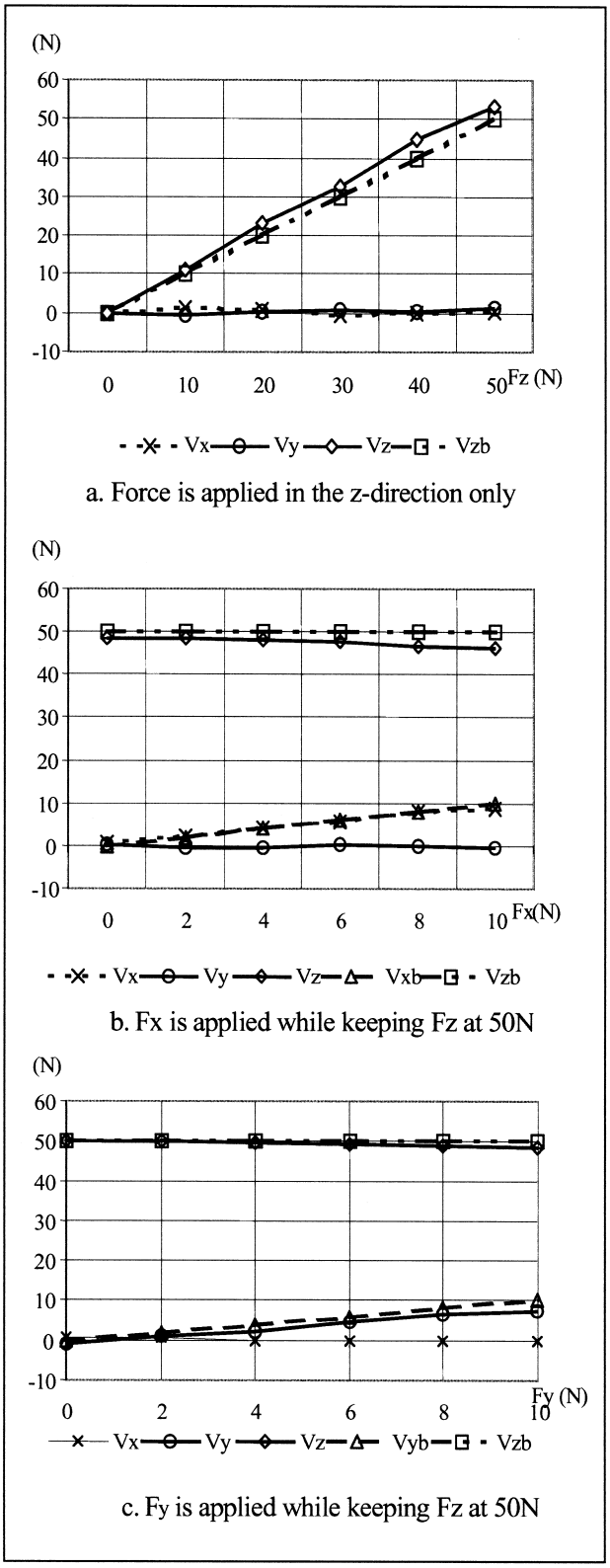

Fig. 13. Input–output relationship of the three force components. (Note 1: Vx, Vy, and Vz are the ideal output curves. Note 2: Vxb, Vyb, and Vzb are the errors which are amplified by 10 times for clearness. Note 3: The output from the sensor have been mapped to forces by a neural net.)

center of the column surface to prevent sliding (see Fig. 2). A set of sensitivity data for every cell in the array for the three force directions was obtained using this method. The sensitivity of the sensing cells were about 13 mV/N in the Z direction and about 2.3 mV/N in the X and Y directions.

The sensitivity of the individual sensing cells was affected by the silicone rubber layer covering the force concentrating columns. An artificial neural network was used to compensate the change, since theoretical analysis of the sensitivity change would be very complex. The neural network was a back-progression network with 97 input neurons, 32 hidden neurons and 3 output neurons. The 97 input neurons received the 32 three-dimensional forces and a temperature-sensing signal from the sensing array. A diode was integrated in the sensing circuit to detect the chip temperature for temperature compensation. The three outputs gave the total tactile forces in the three force directions. The mechanical analysis of the multilayer structure including the rubber layer, the E-shaped membrane and silicon glue is an undergoing research issue. The tactile sensor was connected to the artificial neural network and trained by applying weights on the sensing surface directly. The tactile sensor achieved 2% FS accuracy for total tactile force measurements in the force range of 0 to 50 N for F_z and -10 to 10 N for F_x and F_y (Fig. 13).

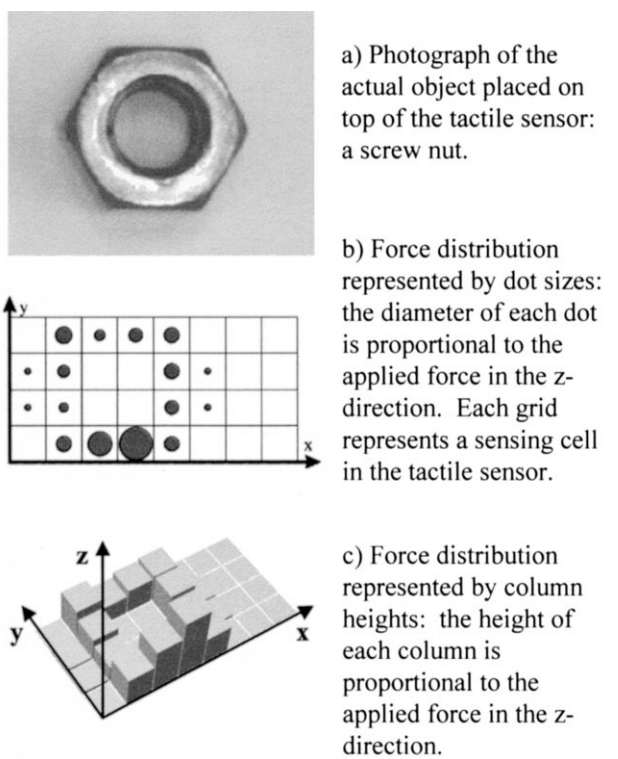

Fig. 14. Tactile image of a screw-nut represented by dot sizes (b) and column heights (c). Each grid represents force output data from a sensing cell in the tactile sensor.

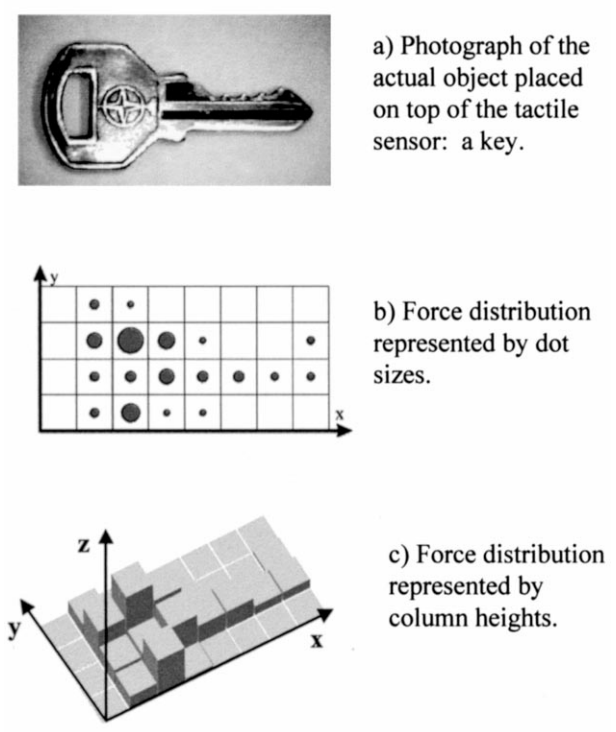

Fig. 15. Tactile image of a key (see Fig. 14 for explanations on dot sizes and column heights).

Some samples, such as keys, weights and screw nuts, were pressed to the tactile sensor to obtain tactile images.

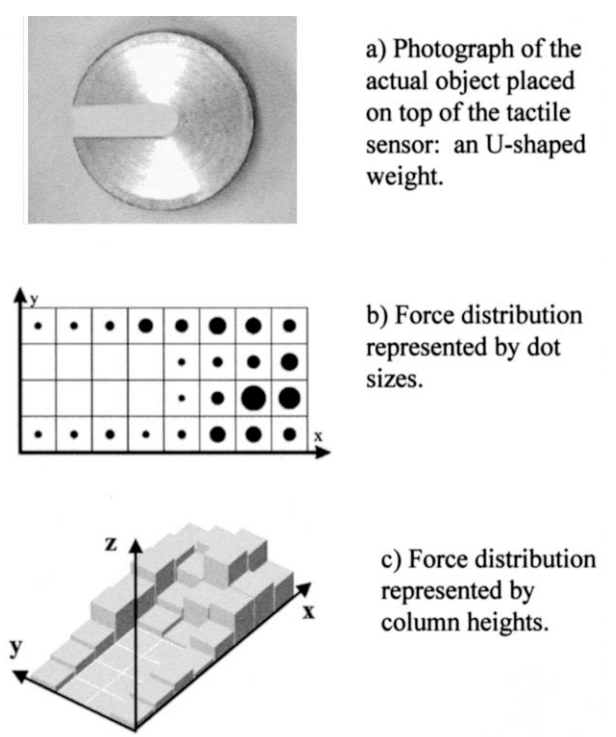

Fig. 16. Tactile image of a U-shaped weight (see Fig. 14 for explanations on dot sizes and column heights).

Good correspondence between the sample shapes and the force distribution were observed as shown in Figs. 14–16.

5. Conclusion

An integrated three-dimensional tactile sensor with large force range and overload-protection function was fabricated using MEMS and standard COMS technology. The sensor cells have integrated piezoresistors, detection circuits, and analogue switches for data readout. Reasonable detection accuracy of three force directions, tactile image correspondence, and the overall tactile sensor compactness and robustness were achieved. Integration of the tactile sensor is underway to a space test-bed robotic system.

Acknowledgements

We would like to thank the Hong Kong UGC (Research Direct Grant #2050173) and High Technology Program of China for funding this research project.

References

[1] B.L. Gray, R.S. Fearing, A surface micromachined microtactile sensor array, Proceedings of IEEE International Conference on Robotics and Automation, Minneapolis, MN, April 1996, pp. 1–6.
[2] K.K. Choi, S.L. Jiang, Z. Li, Multifingered robotic hands: contact experiments using tactile sensors, Proceedings of the 1998 IEEE International Conference on Robotics and Automation, Leuven, Belgium, May 1998, pp. 2268–2273.
[3] B.J. Kane, M.R. Cutkosy, G.T.A. Kovacs, CMOS-compatible traction stress sensor for use in high-resolution tactile imaging, Sens. Actuators, A 54 (1996) 511–516.
[4] Z. Chu, P.M. Sarro, S. Middelhoek, Silicon three-axial tactile sensor, Sens. Actuators, A 54 (1996) 505–510.
[5] M. Ohka et al., A three-axis optical tactile sensor (FEM contact analyses and sensing experiments using a large-sized tactile sensor), Proceedings of IEEE International Conference on Robotics and Automation, Aichi, Japan, May 1995, pp. 817–824.
[6] J.R. Wertz, W.J. Larson, Reducing Space Mission Cost, Microcosm Press and Kluwer Academic Publishers, 1996.
[7] T. Mei, Y.S. Xu, W.H. Liao, W.J. Li, Space microrobots: why, what, and how, Second International Workshop on Micro Robotics and Systems, Beijing, China, October 1998, pp. 222–225.

Biographies

Prof. Tao Mei is currently the Acting Director of the Institute of Intelligent Machines, Chinese Academy of Sciences, Hefei. He has published over 30 scientific papers on MEMS and chemical sensors since 1985. He has won numerous scientific and government awards including the Excellent Paper Prize (1997) awarded by the Fifth National Conference on Sensors and Transducers, Honor Certificate for Outstanding Contribution in Space Science (1997) awarded by the Space Technology Bureau of National Commission of Defense Science and Industry, and the Third Prize for the Progress in Science and Technology of Chinese Academy of Sciences. He was a visiting scholar at the Robot and Automation Center in Middlesex Polytechnic, UK from 1986 to 1987, and was a visiting scientist at the Robotics Institute of the Carnegie Mellon University, USA in 1996. Prof. Mei is currently directing the Engineering Research Centre of Sensing Systems in developing and using MEMS sensors for medical, space robotic, and Internet applications.

Wen J. Li received the BS and MS degrees in Aerospace Engineering from the USC in 1987 and 1989, respectively. His industrial experiences include The Aerospace (1987 to 1995), Silicon Microstructures (summer of 1994), and the Jet Propulsion Laboratory (1995 to 1997). He began his PhD studies at UCLA in 1992, and received his PhD in 1997 specializing in MEMS. Dr. Li joined the faculty of the Department of Mechanical and Automation Engineering of the Chinese University of Hong Kong in 1997. His current research interest is to develop decision-making mechanical structures for biomedical, robotic, and automotive applications.